



## Synthesis and Characterization of Rice Husk Biochar and its Application in the Adsorption Studies of Lead and Copper

Alice Ndekei<sup>1\*</sup>, Muigai-Gitita<sup>1</sup>, Njagi Njomo<sup>2</sup> and Damaris Mbui<sup>2</sup>

<sup>1</sup>Department of Chemistry, J.K.U.A.T, P.O. Box 62000-00200, Nairobi, Kenya.

<sup>2</sup>Department of Chemistry, University of Nairobi, P.O. Box 30197-00100, Nairobi, Kenya.

### Authors' contributions

*This work was carried out in collaboration among all authors. Author AN designed the study, performed the statistical analysis, wrote the protocol and wrote the first draft of the manuscript. Authors MG and NN managed the analyses of the study. Author DM managed the literature searches. All authors read and approved the final manuscript.*

### Article Information

DOI: 10.9734/IRJPAC/2021/v22i430402

#### Editor(s):

(1) Prof. Bengi Uslu, Ankara University, Turkey.

#### Reviewers:

(1) Leong Siew Yoong, University Tunku Abdul Rahman, Malaysia.

(2) Mukilan K, Kalasalingam Academy of Research and Education, India.

Complete Peer review History: <http://www.sdiarticle4.com/review-history/68946>

Original Research Article

Received 26 March 2021

Accepted 03 June 2021

Published 12 June 2021

### ABSTRACT

The present study aimed to use chemically activated rice husk biochar as an adsorbent for the removal of heavy metals from an aqueous solution. A series of the Rice husk biochar (RHB) samples were produced at different temperatures, as follows: 300, 400, 500, 600, and 700°C for 2 hours each through pyrolysis process in Dalhan Scientific Muffle Furnace. The chemically treated rice husk biochar synthesized at 500°C was used as potential char for removal of Cu(II) and Pb(II) from aqueous solutions. The sorption of these metal ions from an aqueous solution was determined after adsorption using Flame Atomic Absorption Spectrophotometry (AAS). The Shimadzu IR Affinity Fourier Transform Infra-Red Spectroscopy (FT-IR) was used for the characterization of rice husk char and it revealed the presence of OH, C=O, and COO<sup>-</sup> bonds which are responsible for heavy metal ions adsorption through chemisorption. The effect of adsorption parameters was determined that is; pyrolysis temperature which was found to be 500°C, the optimal contact time for the metal ions Cu (II) and Pb (II) was found to be 60 minutes, the optimum dosage was 0.250 g and optimum initial concentration was 2 mg/l. The kinetics were

\*Corresponding author: E-mail: [andekei@uonbi.ac.ke](mailto:andekei@uonbi.ac.ke), [andekei70@gmail.com](mailto:andekei70@gmail.com);

tested against pseudo-first order and pseudo-second order model as well Langmuir and Freundlich isotherms. Cu(II), adsorption process followed Pseudo-second order kinetics with regression coefficient ( $R^2$ ) 0.9942 and Langmuir isotherm model with  $R^2$  0.9895. For Pb(II), adsorption capacity followed Pseudo-second order kinetics with regression coefficient ( $R^2$ ) 0.99991 and Freundlich isotherm model with  $R^2$  0.96675 optimum equilibrium adsorption capacity of 0.5274 mg/g.

**Keywords:** Biochar; adsorbent; adsorption; kinetics; isotherms.

## 1. INTRODUCTION

Heavy metals are of great concern to the environment, due to their detrimental effects on human health. Lead and Copper are among the common metals which are environmental pollutants when consumed beyond the permitted levels [1]. Various applications of lead include manufacturing of rechargeable batteries, as an antiknock agent in gasoline, in radiation shields, in the making of water pipes, and also in the construction of houses and building roofs [2]. Lead is known to cause reproductive failure and lower the intelligence quotient in children [3]. Furthermore, lead is documented as a carcinogen [3]. Copper is an essential nutrient in the human body. However, the concentration of copper beyond permitted levels leads to nausea, vomiting, headache, diarrhea, liver damage, and heart failure. The main target of copper toxicity is the liver and leads to chronic diseases, heart failure, and brain damage [4]. Various conventional methods have previously been used to remove heavy metal ions from wastewater. They include membrane filtration, electrocoagulation, reverse osmosis, ion exchange, precipitation, and solvent extraction. However, these methods have the drawbacks of the high cost of purchasing and maintenance of the instruments, expensive chemicals are required, and also the formation of chemical sludge [5].

Various plant materials have been used as low-cost biosorbents for the removal of chemical pollutants from water, for example, rice husk and millet corn [6], kenaf fiber [7], Eucalyptus bark [8] and sugarcane bagasse [9]. The process of metal ion adsorption onto the adsorbent surfaces includes various processes such as micro precipitation, chemisorption, and surface adsorption [10]. Biochar (BC) is a stable carbon-rich solid product obtained via the pyrolysis or carbonization processes. This is the direct thermal decomposition of organic materials or biomass under anaerobic conditions at temperatures of less than 700°C. It produces a

mixture of solid (Biochar), liquid (Bio-oil), and gaseous (Syngas) products [11]. Biochars (BCs) are usually made from a range of biomasses that have diverse chemical and physical property. The biochar has the ability to adsorb metal ions as a result of electrostatic forces between the negative functional groups in the carbon and the positively charged metal ions [12].

Adsorption isotherms are used to describe the equilibrium created between the adsorbate concentration on the solid surface and the adsorbate concentration in solution, at a certain constant temperature. Kinetic studies aid in the determination of the path taken during the adsorption; they are also useful in determining the mechanism and the rate of the adsorption process.

The negative hypothesis of the present study is, the Microporous biochar derived from rice husk does not have high efficiency and adsorptive capacity for removal of lead and copper metal ions from contaminated water.

The objectives of this study were to synthesize and characterize the rice husk biochar and to optimize sorption parameters such as pyrolysis temperature, adsorbent dosage, contact time, and initial metal ions in Pb(II) and Cu(II) ions, and then fit the data into adsorption isotherms and kinetic models.

## 2. MATERIALS AND METHODS

### 2.1 Sample Preparation

The rice husks were washed thoroughly with tap water to remove mud and other water-soluble impurities and rinsed with distilled water. They were then air-dried under shade for 5 hours and then oven-dried at 105°C for 24 hours. The dried rice husks were cut into small pieces of about 10 mm, ground, and then placed into a porcelain crucible each tightly covered with a fitting lid to get rid of the oxygen, and then placed in a Muffle Furnace for the pyrolysis process. The rice husk

biochar samples were obtained at different temperatures, viz: 300, 400, 500, 600, and 700°C for 2 hours each. This assisted in the identification of the optimal temperature for the production of quality and efficient activated carbon. The synthesized biochar samples were stored in air-tight containers for further analysis.

## 2.2 Chemical Activation of Rice Husk Biochar (RHBT)

The adsorption efficiency of the rice husk biochar was increased through chemical activation with 0.1M NaOH to leach down the ash which causes hindrance in pores development. After ash removal from the rice husk char, the biochar was washed and dried in the oven for 24 h. The rice husk char was further activated with ZnCl<sub>2</sub> solution by soaking it, for 24 hours and then thoroughly washed with distilled water until pH 7.0 was obtained. This was done for modification of the surface to increase micro porosity [7].

## 2.3 Optimization of Adsorption Parameters

All analyses for the optimization of adsorption parameters were done in triplicate as follows: optimization of pyrolysis temperature, contact time, adsorbent dosage, and initial metal ions concentration, and the mean values were used in data analysis. In optimization of pyrolysis temperature, 0.125 g of chemically activated chars produced at different temperatures were accurately weighted with analytical balance and put in 100 ml conical flasks. 20 ml of synthetic pollutants of 1 mg/l, 2 mg/l, and 4 mg/l of Cu<sup>2+</sup> and Pb<sup>2+</sup> were added respectively each at a time and agitated at a speed of 200 rpm in an orbital shaker for 30 minutes. The suspensions were filtered and the filtrates were transferred into plastics reagent bottles and were analyzed using the Atomic Absorption Spectroscopy (AAS).

The same procedure was repeated to optimize the other parameters by varying the conditions of the parameter to be determined while holding the other conditions constant. The condition that gave the maximum adsorption uptake was considered to be optimal and helps to proceed to the next stage.

## 2.4 Equilibriums and Kinetic Studies

### 2.4.1 Langmuir isotherm

The Langmuir is a monolayer adsorption isotherm which is based on the assumption that

all the adsorption sites are equals and during adsorption of the adsorbate onto the adsorbent surface, each metal ion occupies a single adsorption site therefore, no interactions between adsorbed species, and no transmigration of adsorbate species in the plane of the surface due to uniform adsorption energy [13]. The linearized form of Langmuir isotherm is;

$$\frac{C_e}{q_e} = \frac{1}{K_L q_m} + \frac{C_e}{q_m} \quad (1)$$

Where,  $q_m$  is the maximum adsorption capacity and  $K_L$  is the Langmuir constant. Langmuir isotherm plot of  $C_e/q_e$  against  $C_e$  were used to obtain  $\frac{1}{q_m}$  and  $K_L$  from the slopes and intercept respectively.

### 2.4.2 Freundlich isotherm

Freundlich is a multilayer isotherm, used to describe the adsorption of adsorbate onto the heterogeneous surface of the adsorbent. The linearized form of Freundlich isotherm is as follows:

$$q_e = K_f(C_e)^{1/n} \quad (2)$$

Taking the logarithm on both sides gives:

$$\log q_e = \log K_f + \frac{1}{n} \log C_e \quad (3)$$

Where,  $q_e$  is the adsorbed amount in mg/g,  $K_f$  and  $n$  are Freundlich constants and  $C_e$  is the equilibrium concentrations in mg/l. For Freundlich isotherm the values of  $K_f$  and  $\frac{1}{n}$  can be obtained from the slope and intercept of the plot of  $\log(q_e)$  against  $\log(C_e)$  [14].

The adsorption isotherms of Langmuir and Freundlich in the adsorption of Cu<sup>2+</sup> and Pb<sup>2+</sup> were obtained with some modification of procedure from the previous studies. The experiment was carried out by varying the amount of adsorbent dose from (0.125 g, 0.250 g, 0.50 g, and 1 g). The optimal parameters previously obtained were used which are: pyrolysis temperature was 500°C, contact time 60 minutes for both copper and lead, dosage for both metal ions were 0.250 g, and initial metal ions concentration for both metals was 2mg/l. 20 ml of concentration of 2 mg/l copper and lead were transferred to 100 ml conical flask and added to the adsorbent dose each at a time. They were agitated at a speed of 200 rpm in an

orbital shaker at the optimal contact time for each metal ion. The filtrates were stored in plastic containers for further analysis.

## 2.5 Pseudo-First Order Kinetics

Pseudo- first order kinetics model predicts that the rate of metal ions intake onto the adsorbent surface increases with an increase in the number of adsorbent binding sites. The linear form of pseudo-first order is;

$$\ln(q_e - q_t) = \ln q_e - K_1 t \quad (4)$$

Where,  $q_e$  (mg/g) and are the adsorption capacity at equilibrium and at time  $t$  (min) respectively and  $q_e$  is the concentration of heavy metal adsorbed  $K_1$  (min<sup>-1</sup>) is the Pseudo-first order rate constant of adsorption. The value of  $K_1$  and  $q_e$  are calculated from the slope and intercept respectively of the linear plot of  $\ln(q_e - q_t)$  versus  $\ln q_e$  [15].

## 2.6 Pseudo-Second Order Kinetics

The Pseudo-second order model predicts that the process of heavy metal adsorption involves the exchange of electrons between the metal ions and the adsorbent and consequently leading to the formation of a chemical bond [15]. The linearized form of Pseudo-second order kinetics is;

$$\frac{t}{q_t} = \frac{1}{K_2 q_e^2} + \frac{t}{q_e} \quad (5)$$

Where,  $K_2$  is the pseudo-second order rate constant and has the units of (g/mg/min). A plot of  $t/q_t$  versus time in minutes is used to obtain the values of  $q_e$  and  $K_2$  from the slope and intercept respectively [16].

The adsorption kinetics, the Pseudo-first order and Pseudo-second order of heavy metal ions removed by rice husk biochar was investigated using optimum conditions obtained at pH 7.0 where batch experiments were carried out by shaking 0.250 g of rice husk biochar with 20 ml of copper and lead into the concentration of 2 mg/l respectively at room temperature. The suspension was agitated at 200 rpm during variable time ranging from 0, 3.75, 7.5, 15, 30, 60 to 120 minutes by doubling the time. The filtrates

were separated using filter paper and stored in plastic containers for further analysis.

All the metal ions' concentrations in the filtrates were analyzed using the Atomic Absorption Spectroscopy (AAS). The % removal of metal ion and amount of metal ion adsorbed on Rice husk biochar ( $Q_e$ ) were calculated by using Equations 6 and 7, respectively:

$$E (\%) = (C_o - C_e) \times 100 \quad (6)$$

where  $C_o$  = the initial (equilibrium) concentrations of the metal ion in solution.

$C_e$  = the final (equilibrium) concentrations of the metal ion in solution.

E% =Removal Efficiency in percentage

Adsorption capacity ( $Q_e$ ) after reaching equilibrium was calculated using equation (7)

$$\text{Adsorption capacity } Q_e = (C_o - C_e) V/W. \quad (7)$$

Where,  $V$  is the volume (L) of solution and  $W$  is the mass (g) of rice husk biochar (RHB).

## 2.7 Determination of Functional Groups of the Biochar

The potassium bromide pellets were prepared by grinding 10 mg of activated rice husk biochar with 250 mg of potassium bromide (FT-IR grade) and pressed at a pressure of 75 kN cm<sup>-2</sup> to a fine powder for 3 minutes. The FT-IR scanning range was set at 400 to 4000 cm<sup>-1</sup> while the spectral resolution was 4 cm<sup>-1</sup>.

## 3. RESULTS AND DISCUSSIONS

### 3.1 Analysis of Functional Groups in the Unpyrolyzed and Pyrolyzed Rice Husk Biochar Before and After Loading with Heavy Metal Ions

The characterization of rice husk biochar products and raw rice husk by using FT-IR helps to identify the enrichment of char surface with functional groups which play a vital role in the adsorption of metal ions. Fig. 1 and 2 are for the unpyrolyzed rice husk and pyrolyzed rice biochar spectra produced at optimum temperature before loading with metal ions.

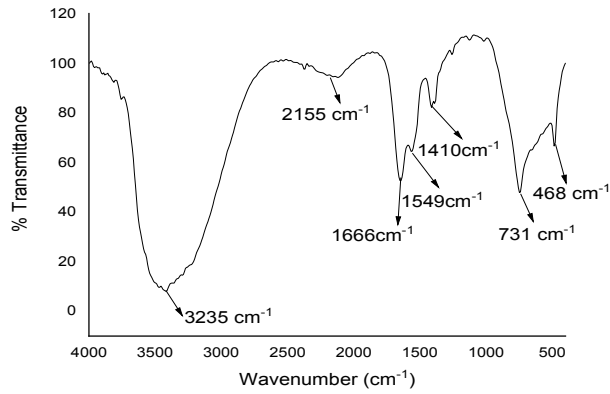


**Fig. 1. FT-IR spectra for the unpyrolyzed rice husk**

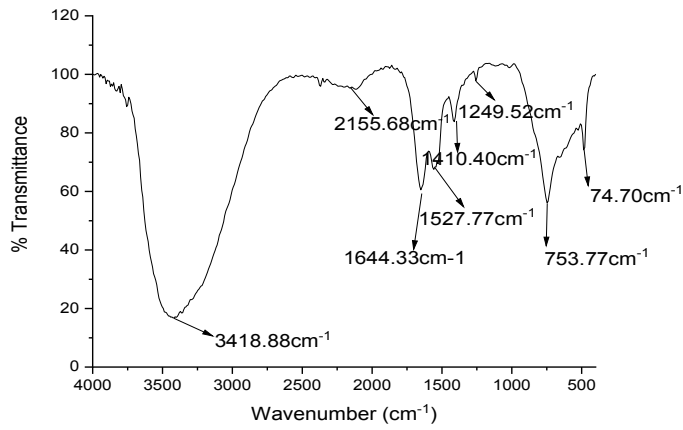


**Fig. 2. FT-IR spectra for the optimum rice husk (RHBT 500)**

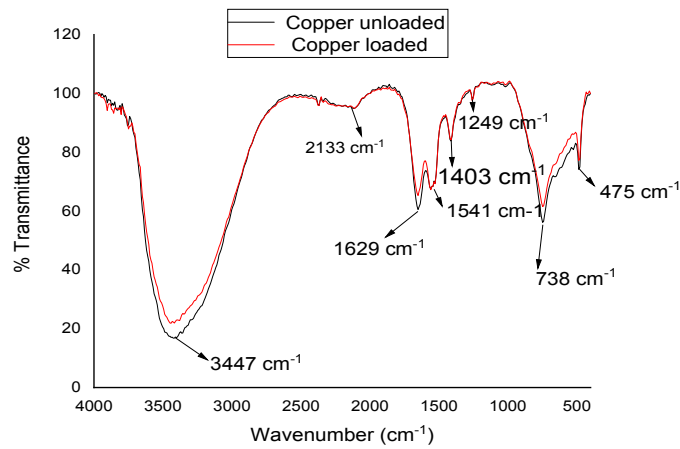


**Fig. 3. FT-IR spectra for copper loaded and unloaded rice husk biochar**

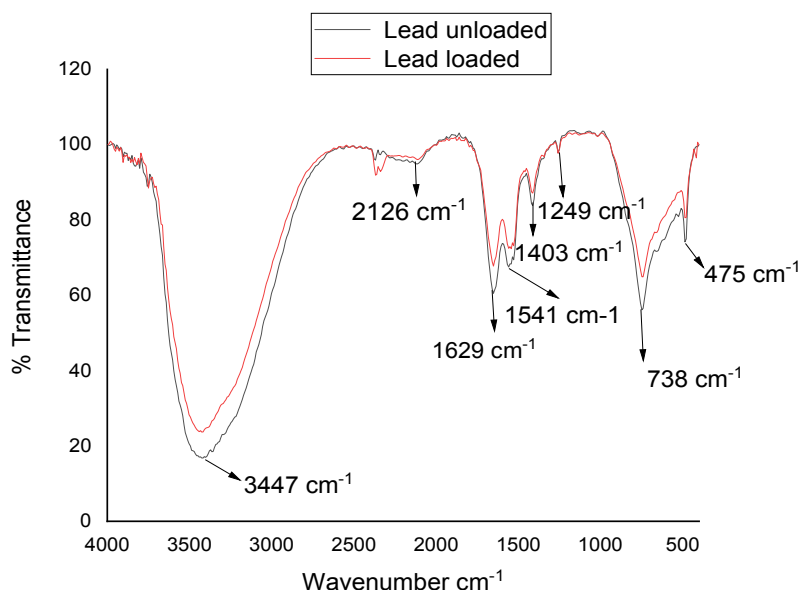


**Fig. 4. FT-IR spectra for lead loaded and unloaded rice husk biochar**

The FT-IR spectrum for unpyrolyzed rice husk and optimum rice husk biochar before loading with Pb(II) and Cu(II) are shown in Figs. 1 and 2. The Unpyrolyzed rice husk displayed several peaks which indicated the complex nature of the adsorbent as in Fig. 1. The broad absorption band at  $V_{\max}$  3235  $\text{cm}^{-1}$  and 3447  $\text{cm}^{-1}$  were assigned to the OH stretching vibrations in organic acids and phenols [17]. The vibrational band at 2155  $\text{cm}^{-1}$  was assigned to the C=O stretch indicating the presence of an aliphatic aldehyde. The band at  $V_{\max}$  1629  $\text{cm}^{-1}$ , 1644  $\text{cm}^{-1}$  and  $V_{\max}$  1666  $\text{cm}^{-1}$  in rice husk was associated with C=O stretching vibrations present in ketones, esters, amides, and carboxylic acids [18]. The band at  $V_{\max}$  1541  $\text{cm}^{-1}$  was associated with N-O stretching vibration for nitro compounds [18]. The band at  $V_{\max}$  1549  $\text{cm}^{-1}$  and  $V_{\max}$  1527  $\text{cm}^{-1}$  were associated with C=C stretching vibration indicating lignin and aromatic carbon. The absorption bands at  $V_{\max}$  1403  $\text{cm}^{-1}$  and  $V_{\max}$  1410  $\text{cm}^{-1}$  were assigned to COO<sup>-</sup> stretching vibrations in esters and carboxylic acids [19]. The band at  $V_{\max}$  between 770 -730  $\text{cm}^{-1}$  was associated with -C-H stretching vibration of long-chain methyl rock. The bands around  $V_{\max}$  468 - 475  $\text{cm}^{-1}$  were assigned to SiO<sub>2</sub> as it is a major component in the chemical structure in rice material and also protects the plant carbon from degradation [9]. The Comparison of FT-IR spectra of unpyrolyzed and pyrolyzed optimal rice biochar loaded with Pb(II) and Cu(II) as shown in Figs. 3 and 4 indicated that, there was

a shift from the original band at  $v_{\max}$  3447  $\text{cm}^{-1}$  to 3235  $\text{cm}^{-1}$ .  $V_{\max}$  2155  $\text{cm}^{-1}$  to 2133  $\text{cm}^{-1}$  and 2126  $\text{cm}^{-1}$ , 1666  $\text{cm}^{-1}$  to 1629  $\text{cm}^{-1}$ ,  $V_{\max}$  1549  $\text{cm}^{-1}$  to 1541  $\text{cm}^{-1}$  and  $V_{\max}$  1410  $\text{cm}^{-1}$  to 1403  $\text{cm}^{-1}$ . There was the appearance of a new band at  $V_{\max}$  1249  $\text{cm}^{-1}$  which indicates the vibration of the C-N bond [14]. The peaks after heavy metals ions adsorption shows the reduction in the intensity. Therefore, the results reveal that there was interaction between the metal ions and the C=O, C=C, O-H, -C-H, N-O and COO<sup>-</sup> functional groups [20,21].

### 3.2 Optimization of Pyrolysis Temperature in the Production of Rice Husk Biochar for Adsorption of Pb(II) and Cu(II)

Pyrolytic temperature is one of the most important process parameters for achieving the best biochar which has already gone complete carbonization for efficient and effective metal ions contaminants removal [22]. The percent metal ions adsorbed were investigated using different samples of rice husk biochars produced at different temperatures. The initial concentration of Pb(II) and Cu(II) metal ions were varied to obtain the optimum char which is more efficient and effective. The results for optimization of pyrolytic temperatures are depicted in Figs. 5 and 6.

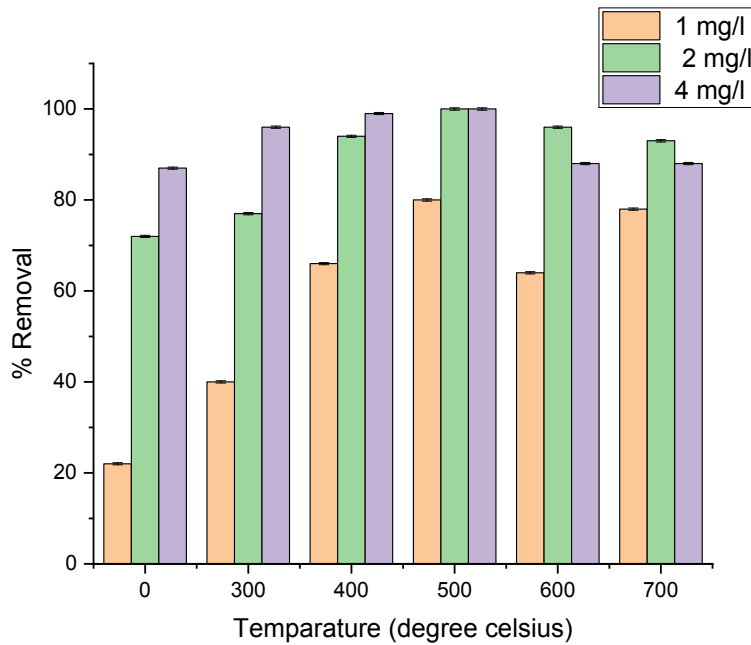


**Fig. 5. Effects of pyrolysis temperature on copper (II) removal**

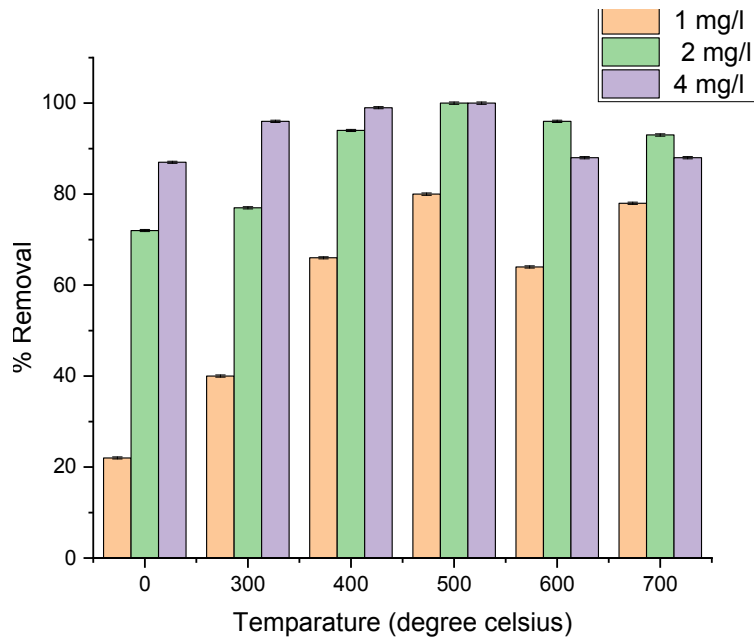


**Fig. 6. Effects of Pyrolysis Temperature on Lead (II) removal**

The optimum pyrolysis temperature which synthesizing the best char for removal of Cu(II) and Pb(II) was found to be 500°C at all the three initial concentrations and was investigated at different temperatures as indicated in Figs. 5 and 6. The increase in heavy metal ions adsorption

with the increase in the pyrolysis temperature was attributed to the decomposition of organic matter, which subsequently led to the increase in the surface area and the size of the pores [23]. Above the optimum temperature, which is 500°C, there was a reduction in heavy metal ions

adsorption for Cu(II) removal at the initial concentration of 1 mg/l and Pb(II) removal at initial concentrations of 1, 2, and 4 mg/l. [24] indicated that this was attributed to the decrease in average pore size, blockage of pores, gradual development of mesopores on the surface of biochar.

### 3.3 Effects of Contact Time on Pb(II) and Cu(II) Removal

The contact time is an important parameter in the adsorption process and was done using the optimum char (RHBT500) for the removal of lead and copper metal ions at different concentrations as indicated in Figs. 7 and 8. The other parameters were held constant.

The effect of contact time on Cu(II) and Pb(II) removal was evaluated at three different initial concentrations of 1, 2, and 4 mg/l by varying the

time from 0 to 120 minutes. It was observed that heavy metal ions' adsorption increased with the increased contact time, this could be due availability of binding sites. The optimum contact time was found to be 60 minutes for Cu(II) and Pb(II) removal at all initial concentrations of 1, 2, and 4 mg/l. The increase in heavy metal ions removal with increased residence time was attributed to the availability of many binding sites and hence the metal ions bound to the adsorbent surfaces [25]. As the optimum residence time was attained, the rate of adsorption became constant, most probably since the number of binding sites became limited, leading to the formation of repulsive forces between the metal ions in the adsorbent surface and the metal ions in the solution [26]. Ultimately all the metal ions were adsorbed as can be seen from the 100% adsorption in all the cases, apart from the 1 mg/l lead and 4 mg/l copper system.

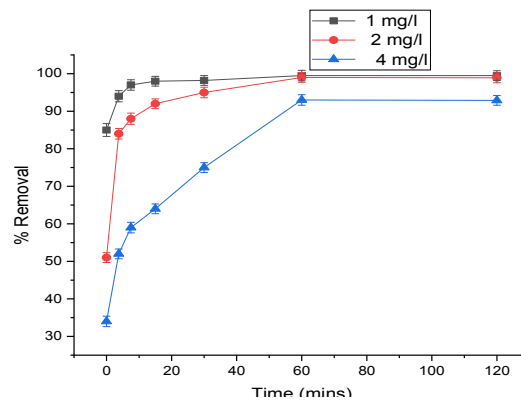


Fig. 7. Effect of contact time on Cu(II) removal

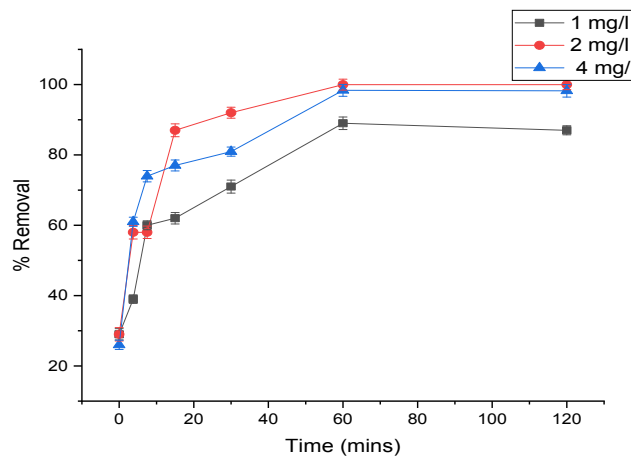
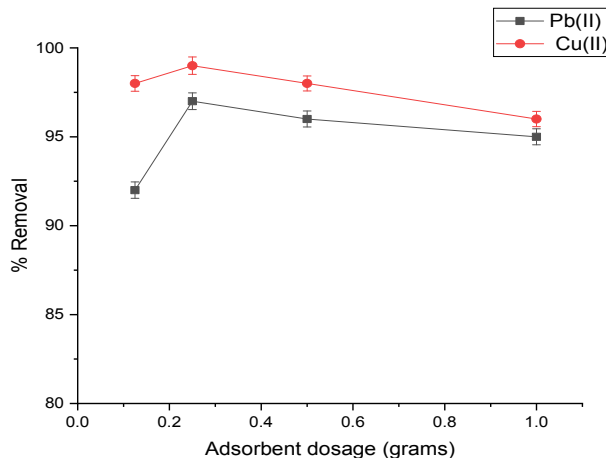


Fig. 8. Effect of contact time on Pb(II) removal





**Fig. 9. Effect of sorbent mass on cu(II) and Pb(II) removal**

### 3.4 Effect of Adsorbent Dosage on Cu(II) and Pb(II) Removal

The ideal dosage of char plays a vital role in the enhancement of effective and efficient removal of contaminants because adsorption is usually influenced by the dosage of adsorbent depending on the availability of binding sites.

The effect of sorbent mass on Cu(II) and Pb(II) removal was evaluated in the range of 0.125 to 1 g by doubling the weight. The optimum dosage for Cu(II) and Pb(II) was found to be 0.250 g with a percentage (%) removal of 99.36% and 97.03% respectively as shown in Fig. 9. An increase in metal ions adsorption with the increase in adsorbent dosage was attributed to an increase in the number of metal ions attachment sites leading to increased interaction between the metal ions and the adsorbent surfaces [20]. At optimum dosage, the percentage of metal removal was almost unchanged and the adsorption amount keeps on decreasing, the same results corresponded to [23]. This was because there is a fixed amount of biomass that a certain adsorbent can adsorb [27].

### 3.5 Effects of Initial Metal Ions Concentration on Cu(II) and Pb(II) Adsorption

The metal ions concentration is the chief driving force in overcoming mass transfer resistance of metal ions between the aqueous solution and the adsorbent surfaces of the rice husk biochar [28].

The effect of Cu(II) and Pb(II) adsorption was evaluated at 4 initial concentrations of 1, 2, 4, and 8 mg/l. From Fig. 10, it was observed an increase in metal ions removal with an increase in initial metal ion concentration. This was because an increase in metal ions concentration is the chief driving force in overcoming mass transfer resistance of metal ions between the aqueous solution and the adsorbent surfaces of the rice husk biochar. Decrease in percentage metal ions removal with an increase in initial metal ion concentration was because, at low initial concentrations of Cu(II) and Pb(II) the ratio of the metal ions binding sites to the total number of metal ions was high, and consequently all the metal ions interacted with the adsorbents surfaces [29]. At high metal ions concentrations, the ratio of the number of metal ions binding sites to the total number of metal ions reduced leading to the decrease in the percentage of metal ions removal [30].

### 3.6 Adsorption Isotherms

Adsorption isotherms are used to describe the equilibrium between the adsorbate concentration on the adsorbent surface and the adsorbate concentration remaining in the solution [31]. In order to determine the adsorption process and the maximum adsorption capacity of the rice husk biochar, the adsorption data were fitted into the Freundlich and Langmuir isotherms.

### 3.7 Freundlich Isotherm

Fig. 11 indicates the Freundlich isotherms of  $Pb^{2+}$  and  $Cu^{2+}$  which occurs on multilayer surface after adsorption onto rice husk biochar.

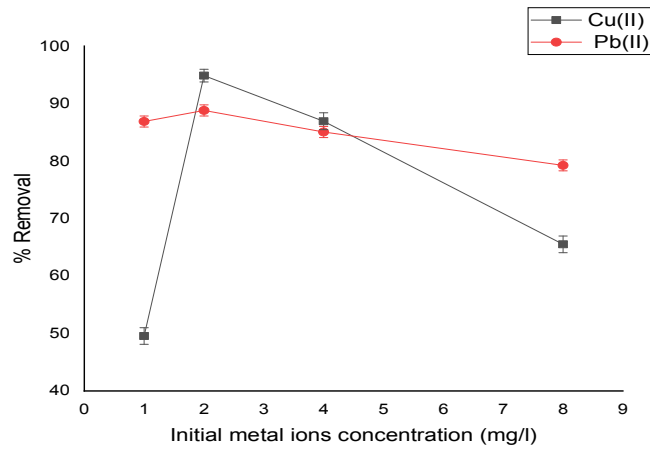


Fig. 10. Effects of initial metal ions concentration on Cu(II) and Pb(II) removal

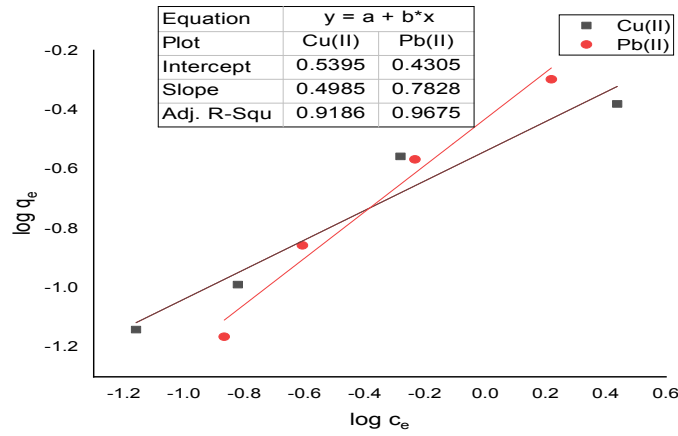


Fig. 11. Freundlich isotherm for Pb(II) and Cu(II) adsorption onto rice husk biochar

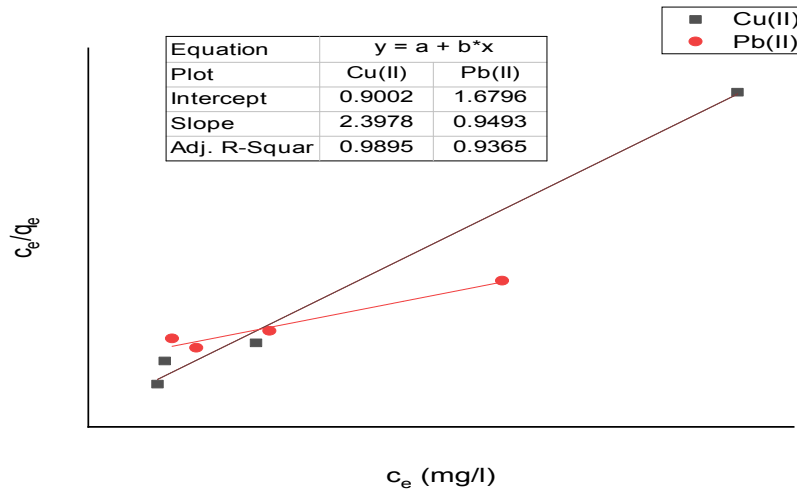


Fig. 12. Langmuir isotherm for Pb(II) and Cu(II) adsorption onto rice husk biochar

**Table 1. Isotherm parameters associated with the adsorption of Pb(II) adsorption**

Freundlich				Langmuir		
$\frac{1}{n}$	n	$K_f$	$R^2$	$\frac{1}{q_{max}}$	$K_L$	$R^2$
0.431	2.32	0.783	0.9675	1.670	0.950	0.9365

**Table 2. Isotherm parameters associated with the adsorption of Cu(II) adsorption**

Freundlich				Langmuir		
$\frac{1}{n}$	n	$K_f$	$R^2$	$\frac{1}{q_{max}}$	$K_L$	$R^2$
0.540	1.85	0.498	0.9187	2.398	0.900	0.9895

### 3.8 Langmuir Isotherm

Fig. 12 indicate adsorption of  $Cu^{2+}$  and  $Pb^{2+}$  onto the char by use of Langmuir isotherm.

For Pb(II) removal results as depicted in Table 1 fitted well to Freundlich isotherm with correlation coefficient ( $R^2$ ) 0.96675 compared with Langmuir with ( $R^2 = 0.9365$ ), implying that for Pb(II) ions removal a multilayer adsorption both on the interior and the exterior surface of the rice husk biochar was prevalent. The experimental data shown in Table 2, Cu(II) removal correlation coefficient ( $R^2$ ) for Langmuir isotherm was 0.9895 while the value of  $R^2$  for Freundlich was 0.9187 implying that monolayer adsorption of Cu(II) ions on the homogeneous surface of the rice husk biochar was the prevalent similar result of copper was reported by [32]. As depicted in Tables 1 and 2 the values of n in Freundlich isotherm signifies the heterogeneous surface in Pb(II) and Cu(II) metal ions because it lies between 1 and 10 indicating a favourable reaction and also a strong bond between adsorbent and metal ions.

### 3.9 Kinetic Studies

Kinetic studies are important in determining the rate of adsorption mechanism and path followed during the metal ions adsorption onto the rice husk biochar. The optimum initial concentration used for both Cu (II) and Pb(II) was 2 mg/l.

#### 3.10 Pseudo-First Order Kinetics

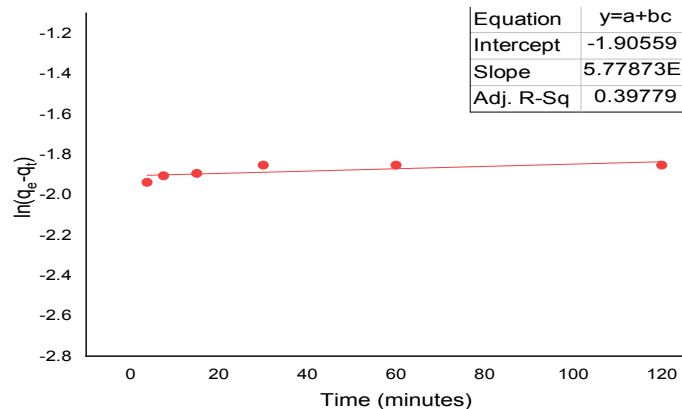
Fig. 13 indicates the Pseudo-first order of  $Cu^{2+}$  onto optimum activated char against time.

Fig. 14 indicates the Pseudo-first order of  $Pb^{2+}$  onto optimum activated char against time.

#### 3.11 Pseudo-Second Order Kinetics

Fig. 15 indicates the Pseudo-second order of  $Cu^{2+}$  onto optimum activated char against time.

Fig. 16 indicates the Pseudo-second order of  $Pb^{2+}$  onto optimum activated char against time.



**Fig. 13. Pseudo-first order kinetics for Cu(II) adsorption**

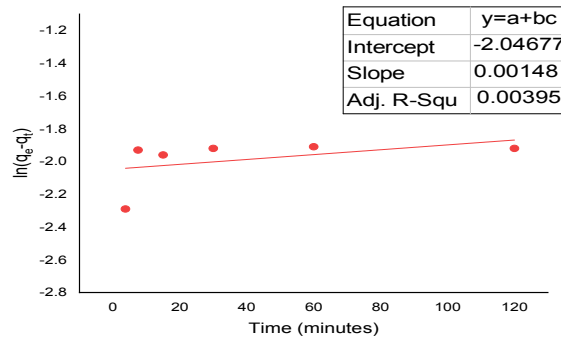


Fig. 14. Pseudo-first order kinetics for Pb(II) adsorption

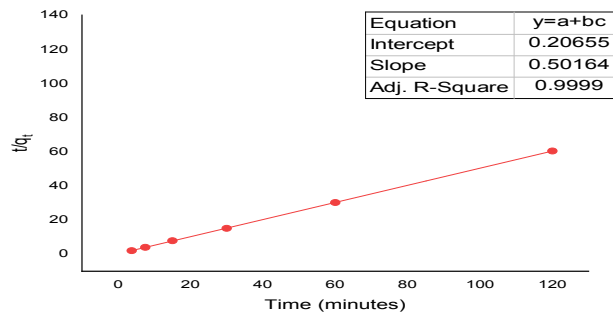


Fig. 15. Pseudo-second order kinetics for Cu(II) adsorption

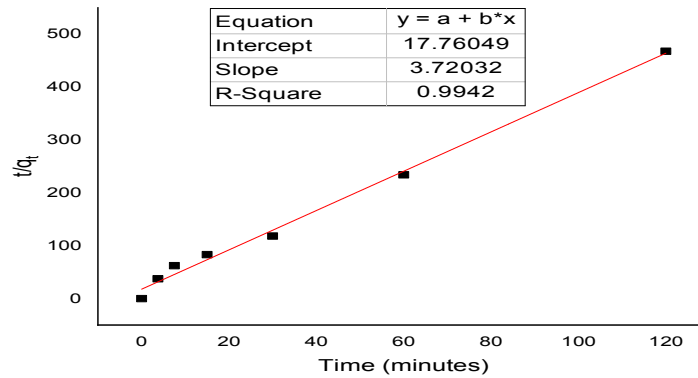


Fig. 16. Pseudo-second order kinetics for Pb(II) adsorption

Table 3. Kinetics parameters associated with the adsorption of Pb(II) adsorption

Pseudo-first order			Pseudo-second order		
$K_1$	$q_e$	$R^2$	$K_2$	$q_e$	$R^2$
0.0015	-2.05	0.0040	0.9326	0.5274	0.9942

Table 4. Kinetics parameters associated with the adsorption of Cu(II) adsorption

Pseudo-first order			Pseudo-second order		
$K_1$	$q_e$	$R^2$	$K_2$	$q_e$	$R^2$
0.577	-1.90	0.3977	0.2065	0.50164	0.9999

The experimental data obtained in this study were fitted to two kinetic models, the Pseudo-first order and Pseudo-second order as fitted in questions 4 and 5. According to regression coefficient ( $R^2$ ) as shown in Tables 3 and 4 the Pseudo-first order did not provide a good description of the sorption process of the  $Pb^{2+}$  and  $Cu^{2+}$  they were very low that is 0.0040 and 0.3977 respectively. The same results corresponded to [15] in the removal of heavy metal ions by use of treated human hair.

The experimental results indicated the biosorption process for both metal ions perfectly comply with Pseudo-second order.  $R^2$  values, as shown in Tables 3 and 4, are very high greater than 0.99. Therefore, the data explained that the rate-limiting step of sorption at all the time involved the chemical sorption due to the formation of the chemical bond between adsorbent and metal ions. Similar results were obtained by [6] in Comparative evaluation for the adsorption of toxic heavy metals onto millet, corn, and rice husks as adsorbents.

#### 4. CONCLUSIONS

The FT-IR spectra indicated that the rice husk biochar is dominated by functional groups as follows: O-H, -C-H, C=C, C=O, N-O, and COO- which participated in heavy metal ions adsorption. Optimum biochar temperature was found to be 500°C, optimum contact time for adsorption of both Cu(II) and Pb(II) at all initial metal ions concentrations of 1, 2 and 4 mg/l was 60 minutes. Optimum adsorbent dosage and initial metal ion concentration for both Cu(II) and Pb(II) removal were found to be 0.25 g and 2 mg/l respectively. Adsorption of Cu(II) onto rice husk biochar was best described by Langmuir isotherm indicating monolayer adsorption on a homogenous material. However, adsorption of Pb(II) was best described by Freundlich isotherm indicating multilayers adsorption on a heterogeneous material. Adsorptions of Cu(II) and Pb(II) ions onto rice husk biochar were well described by pseudo-second order kinetics indicating the formation of chemical bond through the exchange of electrons between the metal ions and the adsorbent. The study established rice husk biochar as an inexpensive method for the removal of Cu(II) and Pb(II) ions from aqueous solutions.

#### ACKNOWLEDGEMENT

The authors wish to acknowledge the following individual and institution for their most valued

assistance; Ephantus Mwangi Kamau in Chemistry Department University of Nairobi and the University of Nairobi Chemistry Department where almost all analyses were done.

#### COMPETING INTERESTS

Authors have declared that no competing interests exist.

#### REFERENCES

1. Khodadadi M, Malekpour A, MA. Removal of Pb (II) and Cu(II) coated magnetic nanopart experimental design Albumin-functionalized removal of Pb (II), Cd (II). *Materials, Microporous and Mesoporous*. 2021; 248:256–265.
2. Šljukić BR, Banks CE, Compton RG. Sono-electroanalysis - Application to lead determination. *Hemijaska Industrija*. 2009;63(5):529–534.
3. Assi MA, Hezmee MNM, Haron AW, Sabri MYM, Rajion MA. The detrimental effects of lead on human and animal health. *Veterinary World*. 2016;9(6):660–671.
4. Araya M, Olivares M, Pizarro F. Copper in human health. *International Journal of Environment and Health*. 2007;1(4):608–620.
5. Al-Baidhani JH, Al-Salihy ST. Removal of heavy metals from aqueous solution by using low cost rice husk in batch and continuous fluidized experiments. *International Journal of Chemical Engineering and Applications*. 2016; 7(1):6–10.
6. Batagarawa SM, Ajibola AK. Comparative evaluation for the adsorption of toxic heavy metals on to millet, corn and rice husks as adsorbents. *Academic Journals Full*. 2019;8(5):1–16.
7. Saeed AAH, Harun NY, Sufian S, Bilad MR, Nufida BA, Ismail NM, et al. Modeling and optimization of biochar based adsorbent derived from Kenaf using response surface methodology on adsorption of  $Cd^{2+}$ . *Water (Switzerland)*. 2021;13(7):1–18.
8. Afroze S, Sen TK, Ang HM. Adsorption removal of zinc (II) from aqueous phase by raw and base modified Eucalyptus sheathiana bark: Kinetics, mechanism and equilibrium study. *Process Safety and Environmental Protection*. 2016; 102:336–352.

9. Maher E Saleh<sup>1</sup>, YAED, Assa FF, Abdesalam<sup>1</sup> AA, Yousef RA. Removal of copper metal ions by sugarcane bagasse and rice. *Science and Technology*. 2020;1–18.
10. Mishra V, Majumder CB, Agarwal VK. Sorption of Zn(II) ion onto the surface of activated carbon derived from eucalyptus bark saw dust from industrial wastewater: Isotherm, kinetics, mechanistic modeling, and thermodynamics. *Desalination and Water Treatment*. 2012;46(3):332–351.
11. Inyang MI, Gao B, Yao Y, Xue Y, Zimmerman A, Mosa A, Pullammanappallil P, Ok YS, Cao X. A review of biochar as a low-cost adsorbent for aqueous heavy metal removal. *Critical Reviews in Environmental Science and Technology*. 2016;46(4):406–433.
12. Vieira MGA, Neto AF, DA, Silva MGC, Carneiro CN, Filho AAM. Adsorption of lead and copper ions from aqueous effluents on rice husk ash in a dynamic system. *Brazilian Journal of Chemical Engineering*. 2014;31(02):519–529.
13. Nworie FS, Nwabue FI, Oti W, Mbam E, Nwali BU. Removal of methylene blue from aqueous solution using activated rice husk biochar: Adsorption isotherms, kinetics and error analysis. *Journal of the Chilean Chemical Society*. 2019;64(1):4365–4376.
14. Mathurasa L, Damrongsiri S. Low cost and easy rice husk modification to efficiently enhance ammonium and nitrate adsorption. *International Journal of Recycling of Organic Waste in Agriculture*. 2018;7(2):143–151.
15. Zhang H, Carrillo-Navarrete F, López-Mesas M, Palet C. Use of chemically treated human hair wastes for the removal of heavy metal ions from water. *Water (Switzerland)*. 2020;12(5):1–17.
16. Lim J, Kang H, Kim L, Ko S. Removal of heavy metals by sawdust adsorption: Equilibrium and kinetic studies. *Environmental Engineering Resource*. 2008;13(2):79–80.
17. Zhao SX, Ta N, Wang XD. Effect of temperature on the structural and physicochemical properties of biochar with apple tree branches as feedstock material. *Energies*. 2017;10(9):1–15.
18. Wang S, Li W, Yin X, Wang N, Yuan S, Yan T, Qu S, Yang X, Chen D. Cd(II) adsorption on different modified rice straws under FT-IR spectroscopy as influenced by initial pH, Cd(II) concentration, and ionic strength. *International Journal of Environmental Research and Public Health*. 2019;16(21):1–15.
19. Daffalla SB, Mukhtar H, Shaharun MS. Preparation and characterization of rice husk adsorbents for phenol removal from aqueous systems. *Science and Technology*. 2020;15(12):1–10.
20. Kariuki Z, Kiptoo J, Onyancha D. Biosorption studies of lead and copper using rogers mushroom biomass 'Lepiota hystrix.' *South African Journal of Chemical Engineering*. 2017; 23:62–70.
21. Pakade VE, Ntuli TD, Ofomaja AE. Biosorption of hexavalent chromium from aqueous solutions by Macadamia nutshell powder. *Applied Water Science*. 2017;7(6):3015–3030.
22. Angin D, Şensöz S. Effect of pyrolysis temperature on chemical and surface properties of biochar of rapeseed (*Brassica napus* L.). *International Journal of Phytoremediation*. 2014;16(8):1–13.
23. Liu L, Deng G, Shi X. Adsorption characteristics and mechanism of p-nitrophenol by pine sawdust biochar samples produced at different pyrolysis temperatures. *Scientific Reports*. 2020; 10(1):1–11.
24. Jia Y, Shi S, Liu J, Su S, Liang Q, Zeng X, Li T. Study of the effect of pyrolysis temperature on the Cd<sup>2+</sup> adsorption characteristics of biochar. *Applied Sciences*. 2018; 8:1–14.
25. Cimá-Mukul CA, Abdellaoui Y, Abatal M, Vargas J, Santiago AA, Barrón-Zambrano JA. Eco-efficient biosorbent based on leucaena leucocephala residues for the simultaneous removal of Pb(II) and Cd(II) ions from water system: Sorption and mechanism. *Bioinorganic Chemistry and Applications*. 2019;1–22.
26. Renu MA, Singh K, Upadhyaya S, Dohare RK. Removal of heavy metals from wastewater using modified agricultural adsorbents. *Materials Today Proceedings*. 2017;4(9):10534–10538.
27. Kareema A, Wael I, Tamer E, Ibrahim M, GY. Chemically modified rice husk as an effective adsorbent for removal of palladium ion. *Science*. 2021;7(1): 1–22.
28. Wang FY, Wang H, Ma JW. Adsorption of cadmium (II) ions from aqueous solution by a new low-cost adsorbent-Bamboo charcoal. *Journal of Hazardous Materials*. 2010;177(3):300–306.

29. Abdel-Fattah TM, Mahmoud ME, Ahmed SB, Huff MD, Lee JW, Kumar S. Biochar from woody biomass for removing metal contaminants and carbon sequestration. *Journal of Industrial and Engineering Chemistry*. 2015; 22:103–109.
30. Komkiene J, Baltreinaite E. Biochar as adsorbent for removal of heavy metal ions [Cadmium(II), Copper(II), Lead(II), Zinc(II)] from aqueous phase. *International Journal of Environmental Science and Technology*. 2016;13(2):471–482.
31. Rasmey AH, Aboseidah A, Youssef A. Phenotypic and molecular characterization of a novel isolate of *Pseudomonas aeruginosa* applicable for biosorption of  $Pb^{2+}$  from waste water: Application of biosorption isotherm models. *Egyptian Journal of Microbiology*. 2018; 53:37–48.
32. Zafar S, Khan MI, Lashari MH, Khraisheh M, Almomani F, Mirza ML, Khalid N. Removal of copper ions from aqueous solution using NaOH-treated rice husk. *Emergent Materials*. 2020;3(6):857–870.

© 2021 Ndekei et al.; This is an Open Access article distributed under the terms of the Creative Commons Attribution License (<http://creativecommons.org/licenses/by/4.0>), which permits unrestricted use, distribution, and reproduction in any medium, provided the original work is properly cited.

*Peer-review history:*

*The peer review history for this paper can be accessed here:*  
<http://www.sdiarticle4.com/review-history/68946>